Molecular Neurobiology
https://doi.org/10.1007/s12035-024-04159-8

ORIGINAL ARTICLE

Neuroprotective Therapeutic Potential of microRNA-149-5p against Murine Ischemic Stroke

Samira Vahidi[1] · Mohammad-Reza Bigdeli[1,2] · Hosein Shahsavarani[3] · Salma Ahmadloo[1] · Mehrdad Roghani[4]

Received: 9 October 2023 / Accepted: 30 March 2024

Abstract

Ischemic stroke resulting from blockade of brain vessels lacks effective treatments, prompting exploration for potential therapies. Among promising candidates, microRNA-149 (miR-149) has been investigated for its role in alleviating oxidative stress, inflammation, and neurodegeneration associated with ischemic conditions. To evaluate its therapeutic effect, male Wistar rats were categorized into five groups, each consisting of 27 rats: sham, MCAO, lentiviral control, lentiviral miR-149, and miR149-5p mimic. Treatments were microinjected intracerebroventricularly (ICV) (right side), and ischemia was induced using middle cerebral artery occlusion (MCAO) procedure. Post-MCAO, neurological function, histopathological changes, blood-brain barrier (BBB) permeability, cerebral edema, and mRNA levels of Fas ligand (Faslg) and glutamate ionotropic NMDA receptor 1 (GRIN1) were assessed, alongside biochemical assays. MiR-149 administration improved neurological function, reduced brain damage, preserved BBB integrity, and attenuated cerebral edema. Upregulation of miR149-5p decreased Faslg and GRIN1 expression in ischemic brain regions. MiR-149 also reduced oxidative stress, enhanced antioxidant activity, decreased caspase-1 and −3 activity, and modulated inflammatory factors in ischemic brain regions. Moreover, DNA fragmentation as an index of cell death decreased following miR-149 treatment. In conclusion, the study underscores miR-149 potential as a neuroprotective agent against ischemic stroke, showcasing its efficacy in modulating various mechanisms and supporting its candidacy as a promising therapeutic target for innovative strategies in stroke treatment.

Keywords Ischemic Stroke · MicroRNA-149 · Oxidative Stress · Inflammation · Cell Death

Introduction

Ischemic stroke (IS), a devastating neurological disorder, is a leading global cause of death and disability [1]. It arises from a blockage in the brain's blood vessels, impeding the delivery of essential oxygen and nutrients. This condition results in neuronal damage, cell death, and a cascade of events that contribute to its debilitating nature [1].

Arterial hypertension stands as a substantial contributor to the risk of ischemic stroke, prompting both vessel rupture and hemorrhagic stroke [2]. The development of atherosclerosis can obstruct arteries, culminating in ischemia of brain regions. Notably, atrial fibrillation assumes the role of a prothrombotic condition. For individuals grappling with atrial fibrillation, the persistent threat of new blood clot formation looms, ultimately culminating in cerebral infarction or stroke [3]. The imperative to prevent stroke within this demographic cannot be overstated, as their susceptibility to clot formation persists at any given instance. As a strategic

✉ Mohammad-Reza Bigdeli
bigdelimohammadreza@yahoo.com

✉ Mehrdad Roghani
mroghani@shahed.ac.ir

1 Department of Animal Science and Marine Biology, Faculty of Life Sciences and Biotechnology, Shahid Beheshti University, Tehran, Iran

2 Institute for Cognitive and Brain Science, Shahid Beheshti University, Tehran, Iran

3 Department of Cell and Molecular Biology, Faculty of Life Sciences and Biotechnology, Shahid Beheshti University, Tehran, Iran

4 Neurophysiology Research Center, Shahed University, Tehran, Iran

Published online: 04 April 2024

measure against stroke risk, a range of approaches are harnessed to shield the brain against potential ischemic events. In the context of thrombosis and embolism, excitotoxicity and cerebral edema assume prominence. While thrombolysis stands as the primary treatment [4], the sphere of brain injury transcends the confines of the affected region. Reperfusion serves as the trigger for inflammation and oxidative stress, thereby fueling secondary brain impairment. The mitigation of inflammation and oxidative stress could potentially avert such damage [5].

Despite substantial strides in comprehending the pathophysiology of stroke, the existing array of treatment choices for this condition remains scarce. Cerebral ischemia/reperfusion (I/R) injury, emblematic of insufficient blood supply followed by subsequent reperfusion, contributes to oxidative stress, exacerbated inflammation, and glutamate excitotoxicity [6]. The intricacy revolves around the identification of effective interventions to forestall compromised neurological functionality stemming from neuronal death in the wake of ischemic stroke. Consequently, the incorporation of therapeutic interventions targeting neuronal death assumes a pivotal role in devising innovative treatment modalities to confront ischemic stroke. As part of the spectrum of measures to thwart the menace of stroke, the harnessing of microRNAs (miRs) emerges as one such avenue aimed at bolstering the brain's resilience against cerebral infarctions.

MiRs are diminutive RNA molecules that govern gene expression and exhibit potential as a therapeutic avenue for ischemic stroke. Research has scrutinized bloodstream miRs as indicators of stroke [5]. Exploring specific miRs and their molecular targets can provide insights into the pathways affected by stroke. These small RNA molecules act as negative regulators of target messenger RNAs, leading to mRNA degradation or translational inhibition. MiRs are also involved in essential biological processes such as cell cycle control, metabolism, apoptosis, and immune response [5]. Despite an incomplete understanding of the link between cerebral I/R injury and miRs, recent research identified some miRs associated with this injury. In acute ischemic stroke patients, novel circulating miRs linked to inflammation, apoptosis, and angiogenesis have been found, suggesting their potential as biomarker and also in therapeutic development [7]. Specifically, downregulated miR-126 in inflammation and upregulated miR-21 in apoptosis may contribute to ischemic stroke pathogenesis, while downregulated miR-137 in angiogenesis may impact blood supply. Overall, miRs show therapeutic promise in ischemic stroke [7].

miR-149, a dysregulated miR found in various diseases including cancer [8], diabetes [9], and cardiovascular diseases [10], has shown neuroprotective effect in ischemic stroke [11]. Studies have demonstrated that level of miR149-5p reduces in models of middle cerebral artery occlusion (MCAO) and oxygen-glucose deprivation/reoxygenation (OGD/R) [11, 12]. Moreover, miR-149 has been shown to play an anti-inflammatory role by directly targeting tumor necrosis factor-α (TNF-α) and interleukin-6 (IL-6) mRNAs, thereby preventing their increase and reducing inflammation [13]. Additionally, miR-149 has been found to regulate blood-brain barrier (BBB) permeability by targeting sphingosine-1 phosphate receptor2 (S1PR2) of pericytes, resulting in decreased BBB leakage [11, 12]. These results imply that miR-149 might hold promise as a viable target for therapeutic intervention in addressing ischemic stroke. Nevertheless, the precise mechanism by which miR-149 reduces complications associated with cerebral ischemia remains to be fully elucidated. Therefore, our aim encompassed the examination of miR-149 influence on oxidative stress, markers of inflammation, cell death, and the ensuing sequelae of MCAO, such as disruption of the BBB, edema, and impairments in neurological function.

Materials and Methods

Animals and Experimental Groups

The animal experiments adhered to the National Institute of Health Guide for the Care and Use of Laboratory Animals and received approval from the Research Ethics Committees of Shahid Beheshti University (IR.SBU.REC.1400.100). Male Wistar rats weighing between 250 and 300 g were sourced from Karaj Institute of Pasteur (Iran). They were housed in a temperature-controlled room ($22 \pm 2^{\circ}$C) with a 12-hour light-dark cycle (light on from 8 a.m. to 8 p.m.) and had unrestricted access to water and specialized pellet food. The rats were randomly assigned to five groups: a sham group (Sham) subjected to surgical stress without ischemic insult, a control group (MCAO) exposed to 1 h of ischemia followed by 24 h of reperfusion, an LV-Control group receiving lentiviral green fluorescent protein, a first treatment group (LV-miR149) receiving lentiviral miR-149, and a second treatment group (miR149-5p) receiving mimic miR149-5p. Each group was further divided into subgroups for evaluating various parameters: TTC ($n=5$) and Nissl ($n=5$) staining for tissue damage, cerebral edema ($n=5$), BBB permeability ($n=5$), Fas ligand (Faslg), and Glutamate Receptor Ionotropic NMDA 1 (GRIN1) mRNA levels ($n=3$), and specific parameters were evaluated using biochemical assays ($n=4$).

Lentiviral Vector Construction and Transduction

The lentiviral vector used for inserting pre-miR-149 was pCDH-CMV-MCS-EF1-cGFP-T2A-Puro. HEK-293T cells (IBRC C10139, Iran) were employed to package the pCDH expression constructs into pseudo-viral particles, following Tiscornia's protocol with calcium phosphate/DNA (BN-0011.19, Iran) [14]. When the HEK-293T cells reached 60-70% confluency, they were transfected with plasmids LV-Control or LV-miR149 (BN-0011.28, Iran). The medium was replaced after 24 h and cell supernatant was collected at 48 and 72-hour post-transfection. Lentiviral vectors were purified, their titer was determined, and validated vectors were used in subsequent experiments.

Stereotaxic Injection

Rats were anesthetized using ketamine (Bremer Pharma GmbH, Germany)/xylazine (Merk, Belgium) (60 mg/kg and 10 mg/kg) and placed in a stereotaxic instrument. Then, LV-Control or LV-miR149 (1.3×10^9 TU/ml, 8 µl) or rno-miR-149-5p mimic (3 µl) (MBS8303269, MyBioSource, USA) was intracerebroventricularly (ICV) (right side) injected at the coordinates determined by the Paxinos Atlas (0.8 mm posterior to Bregma, 1.5 mm lateral to the midline, and 3.5 mm ventral to the surface of the skull) at a rate of 1 µl/min. After 8 days for LV-groups or 24 h for miR mimic, these rats underwent MCAO surgery (Fig. 1).

MCAO Procedure

For the MCAO model, animals were anesthetized with ketamine/xylazine and underwent surgery to induce middle cerebral artery occlusion. A nylon suture was inserted through the External Carotid Artery (ECA) into the Internal Carotid Artery (ICA) until it reached the Anterior Cerebral Artery (ACA), blocking blood flow to the Middle Cerebral Artery (MCA). After 60 min of ischemia, blood flow was restored [15]. Throughout the procedure, rectal body temperature was maintained around 37°C.

Evaluation of Neurological Performance

The neurological status of each group was assessed 24 h after MCAO employing an 18-point rating scale. This comprehensive evaluation encompassed tests for mobility, sensory perception, balance on a beam, absence of reflexes, and identification of abnormal movements. The grading scale ranged from 0 to 18, with zero denoting unimpaired function and 18 signifying the utmost severity of neurological impairment. A detailed description of this behavioral scoring system has been reported by Chen et al. [16].

2,3,5-Triphenyltetrazolium Hydrochloride (TTC) and Nissl Staining

After a 24-hour reperfusion period, the brain was carefully extracted and sliced into 2 mm sections using a brain matrix. Tissue damage was assessed by staining the slices with TTC (Sigma-Aldrich, US) at 37°C for 20 min, followed by capturing digital images [17]. Quantification of damage volume was conducted with ImageJ 1.52v, utilizing a formula involving hemisphere areas.

For histological analysis, brain tissues were fixed in buffered 10% formalin, dehydrated, and embedded in paraffin. Thin 5 µm sections were prepared using a microtome, followed by Cresyl violet staining for further microscopic examination [18]. This evaluation focused on determining

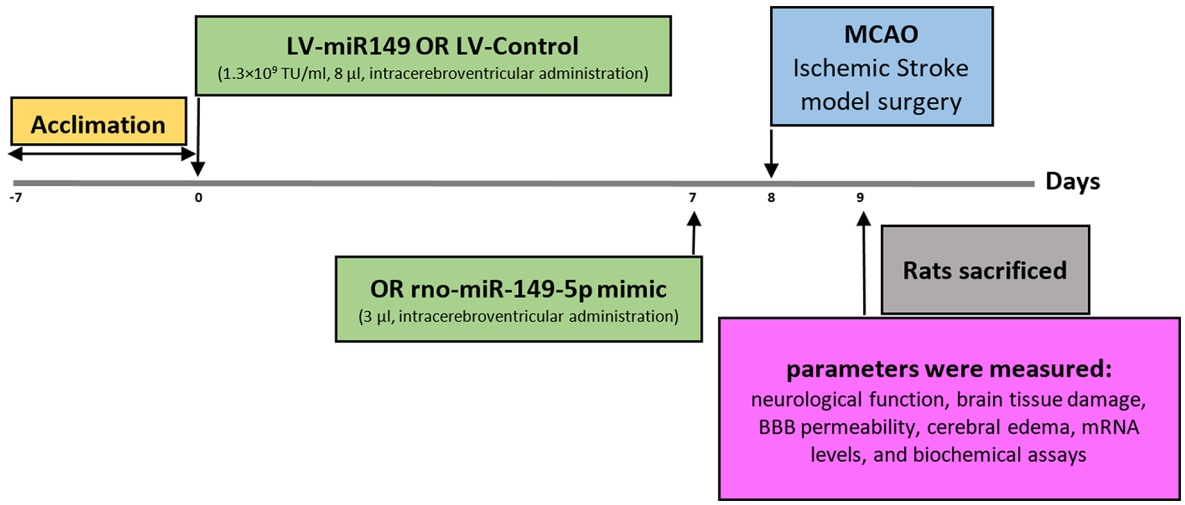

Fig. 1 Schematic experimental design of the study. LV-Control or LV-miR149 (1.3×10^9 TU/ml, 8 µl) or rno-miR149-5p mimic (3 µl) was injected into the intracerebroventricular. Following 8 days for LV-groups or 24 h for the miR mimic group, the rats underwent MCAO model surgery. MCAO, middle cerebral artery occlusion; LV, lentiviral; miR, microRNA

neuronal survival in the cortex, striatum, and piriform cortex regions. Neurons with round shapes, distinct nucleoli, and lightly stained nuclei were categorized as surviving, while shrunken neurons with pyknotic and dark nuclei were identified as dark neurons. The percentage of dark neurons relative to total cells was calculated for each area [19].

Blood-brain Barrier (BBB) Permeability Assessment

A 2% Evans blue dye (Sigma-Aldrich, US) solution was administered intravenously at a rate of 4 ml/kg 30 min after inducing ischemia in animals. After 24 h of reperfusion, a saline solution was injected into the heart until colorless perfusion fluid emerged from the right atrium, indicating clearance of the dye. Brain regions (piriform cortex-amygdala, cortex, and striatum) in the right hemisphere were isolated, weighed, and placed in separate tubes with phosphate-buffered saline. Homogenization, protein precipitation with trichloroacetic acid, and centrifugation were performed. The supernatant's optical absorption at 610 nm was measured with a microplate reader (BioTek 800 TS) to determine dye concentration, using a standard curve [20].

Brain Water Content

Animals were euthanized with deep anesthesia, followed by brain removal and dissection into specific regions. Tissue weights were recorded before subjecting them to 24-hour drying at 120°C (PID-C168 Zist Fanavar, Iran). Moisture content for each part was calculated using the formula: [(wet weight - dry weight) / wet weight] × 100% [11].

Real-Time PCR

To profile mRNA expression, we conducted real-time PCR. The right brain hemisphere was carefully dissected, isolating specific regions such as the piriform cortex-amygdala, cortex, and striatum under ice-cold conditions. Total RNA was extracted from the brain tissues following the guidelines provided by the manufacturer (A101231, Parstous, Iran). Subsequently, the RNA was converted into cDNA using the EasyTM cDNA synthesis kit (A101161, Parstous). Real-time PCR was performed in duplicate using the Step One Plus device (Applied Biosystems) and the RealQ Plus 2x Master Mix Green with high ROX™ (A325402, AMPLIQON, Denmark). The primers listed in Table 1 were employed specifically to target miR149-5p, Faslg, and GRIN1. Small nucleolar RNA, C/D box 87 (SNORD87) (BN-0011.17.5, Bonbiotech, Iran), and glyceraldehyde 3-phosphate dehydrogenase (GAPDH) were used as endogenous controls to normalize the mRNA levels. The $2^{-\Delta Ct}$ method was utilized to calculate the results, ensuring accurate analysis [11].

Table 1 The quantitative real-time PCR primers of miR149-5p, Faslg, GRIN1, and GAPDH

Primer sequence (5'→3')	Genes
Forward: AGTCTGGCTCCGTGTCTTCA	**miR149-5p**
Reverse: CGATCTCTGGTCAGCCTGTG	
Forward: CACCAACCACAGCCTTAGAGTATC	**Faslg**
Reverse: CTCCAGAGATCAAAGCAGTTCCA	
Forward: CCAGATGTCCACCAGACTAAAG	**GRIN1**
Reverse: CCGTACAGATCACCTTCTTCAC	
Forward: GGCAAGTTCAACGGCACAG	**GAPDH**
Reverse: CGCCAGTAGACTCCACGAC	

miR-149-5p microRNA-149-5p; ***Faslg*** Fas ligand; ***GRIN1*** Glutamate Receptor Ionotropic NMDA 1; ***GAPDH*** Glyceraldehyde 3-Phosphate Dehydrogenase

Biochemical Parameters

The cortex, striatum, and piriform cortex-amygdala from the right brain hemisphere were carefully excised and then homogenized in a Tris-HCl buffer solution (150 mM, pH 7.4) while maintaining a cold temperature (4°C) [21]. Following centrifugation (10,000 rpm, 4°C, 10 min), the resulting supernatant was utilized to assess various parameters including nitrite, malondialdehyde (MDA), and glutathione (GSH), as well as the activity of glutathione peroxidase (GPx), glutathione reductase (GR), superoxide dismutase (SOD), catalase (CAT), caspase-1 and − 3, DNA fragmentation, and inflammatory markers such as IL-10, IL-17, and TNF-α.

2.10.1. Nitrite Assay

The Griess method was used to measure nitrite content in the supernatant, detecting nitrite. Griess reagent produced color under acidic conditions. A microplate reader measured absorbance at 540 nm, quantifying total nitrite levels [21].

Determination of MDA Level

Malondialdehyde (MDA), an end product of lipid peroxidation, was measured as an oxidant using the thiobarbituric acid (TBA) assay method. TBA assay kit (Kiazist, Iran) was used to quantify MDA levels at 532 nm wavelength, indicating oxidative damage [22].

Assessment of SOD Activity

Superoxide dismutase (SOD) activity was evaluated utilizing a commercially provided kit (Kiazist, Iran). This method is grounded on SOD's capability to impede the transformation of resazurin into resorufin, facilitated by the xanthine/xanthine oxidase system, which consequently mitigates

superoxide radicals. Subsequently, the absorbance was measured at 570 nm wavelength [22].

Measurement of CAT Activity

Catalase activity was measured by following the manufacturer's instructions (Kiazist, Iran). The experiment involved initiating the reaction, introducing an inhibitor, and assessing the resulting purple color's intensity at 540 nm using an ELISA microplate reader. Specific catalase activity was expressed as U/mg protein [23].

Determination of GSH and GR

Glutathione (GSH) levels and glutathione reductase (GR) activity were ascertained through commercially available kits (Kiazist, Iran) following the guidelines by the manufacturer.

GSH serves as a dependable gauge of the antioxidant potential within biological samples or tissues, given its composition of unoxidized thiol (–SH) groups. Interaction with the Ellman reagent (DTNB) in the presence of these unoxidized or free sulfhydryl groups leads to the creation of a DTNB-sulfhydryl complex, measurable at 405 nm wavelength. Assay outcomes accurately reflect the antioxidant status of the tested samples [22].

GPx Assay

Glutathione peroxidase (GPx) activity was evaluated by Kiazist kit with a reaction involving glutathione reductase and NADPH as a coenzyme. This reaction reduces hydrogen peroxide to water while oxidizing glutathione. Absorbance was measured at 340 nm in kinetic mode and recorded every minute for 5 min [24].

Caspase-1, Caspase-3, and DNA Fragmentation Analyses

Caspase-3 activity, a marker of cell death, was evaluated using a Kiazist kit, while caspase-1 activity as an indicator of pyroptosis was measured with an Abcam, UK kit. The assessment of brain DNA fragmentation, representing apoptosis, was conducted using Roche's Cell Death Detection ELISA Plus kit. All enzyme activities were recorded at 405 nm [25, 26].

TNF-α, IL-10, and IL-17

TNF-α, IL-10, and IL-17 levels in brain tissue were measured using Sandwich ELISA. Antibodies from Santa Cruz Biotechnology were utilized. Microplates were coated with capture antibodies, incubated, and blocked. Samples and standards were added, followed by detection antibodies and subsequent incubation. Optical density was measured at 450 nm using a plate reader. Concentrations were determined through plotted standard curves [27].

Protein Measurement

Protein content was measured using the bicinchoninic acid (BCA) quantification kit by Kiazist. The method relies on proteins reducing copper (Cu^{2+}) to Cu^{+} ions, forming a colored complex at 560 nm, indicating protein quantity [21].

Statistical Analysis

GraphPad Prism software (v9.5.1) was employed for data analysis. Statistical evaluations encompassed either One-Way ANOVA followed by Tukey's post-test or Kruskal-Wallis followed by Dunn-Bonferroni post-test, contingent on the data's characteristics. The outcomes are depicted as mean ± SEM, with statistical significance at $p < 0.05$.

Results

Enhanced Neurological Function Following miR-149 Administration

To investigate the miR-149 influence on stroke outcomes, we used an 18-point scoring system to evaluate neurological function in a rat model of MCAO, as indicated before in the Methods section. The findings revealed a significant increase in the neurological deficit score after subjecting rats to 1 h of cerebral ischemia followed by 24 h of reperfusion, in comparison to sham rats (14.4 ± 0.42 vs. 3.5 ± 0.22) (Kruskal-Wallis test, $p < 0.001$). Additionally, treatment with LV-miR149 (14.4 ± 0.42 vs. 6.8 ± 0.85) ($p < 0.01$) or miR149-5p mimic (14.4 ± 0.42 vs. 8.7 ± 0.67) ($p < 0.05$) resulted in improved neurological function in the MCAO rat model (Fig. 2).

Severe Brain Tissue Injury Induced by MCAO in rats

Staining techniques, such as TTC and Nissl, were utilized to reveal indications of tissue damage in the ischemic brain hemispheres. The MCAO model induced noticeable neurological deficits and neuronal cell death in both cortical and subcortical regions. Treatment involving LV-miR149 (370.2 ± 17.53 vs. 200.8 ± 19.92) ($p < 0.001$) or the miR149-5p mimic (370.2 ± 17.53 vs. 221.5 ± 11.21) ($p < 0.001$) demonstrated a substantial decrease in the total volume of damaged tissue. Specifically, the reduction in stroke volume was markedly pronounced in the

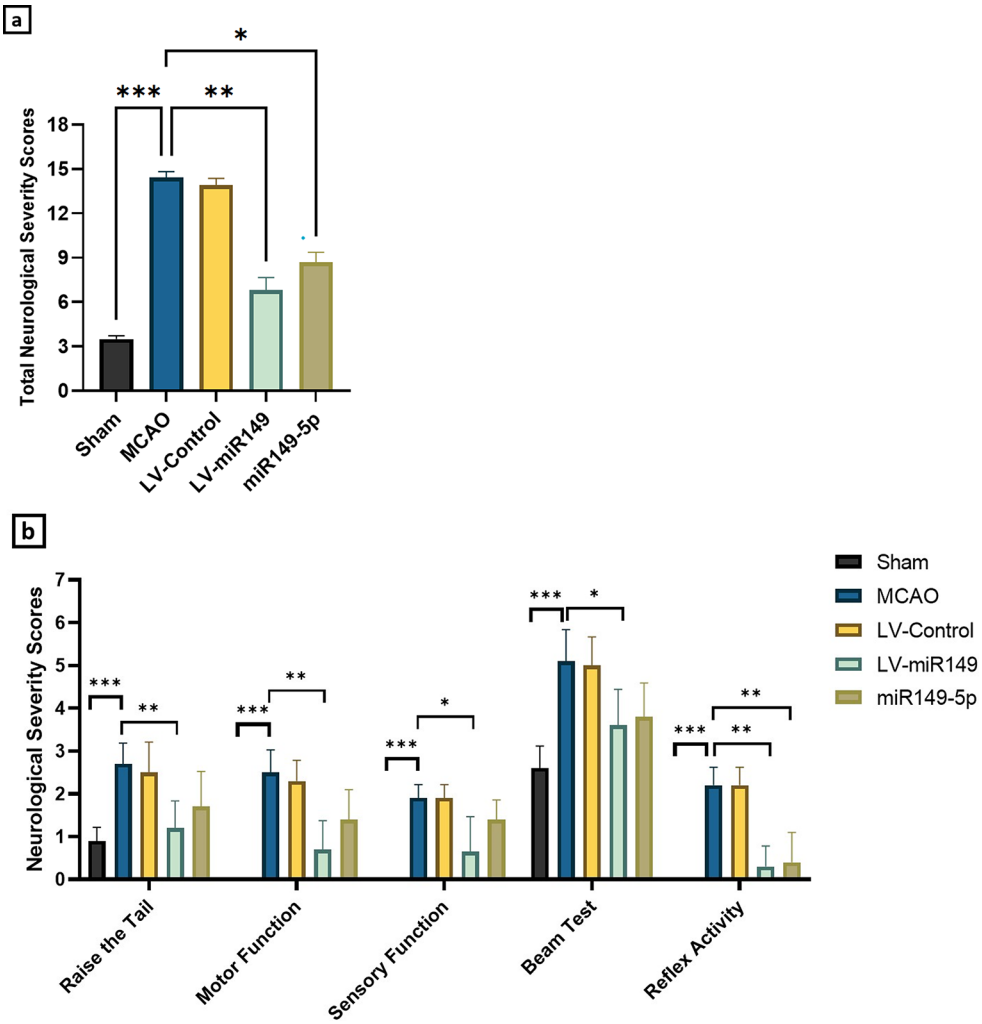

Fig. 2 The effect of miR-149 administration on neurological outcomes was assessed 24 h after inducing ischemic stroke. This evaluation included (**a**) total neurological severity scores and (**b**) individual components of neurological severity scores, such as raising the tail, motor and sensory function, beam test, and reflex activity. The results from Sham, MCAO, LV-control, LV-miR149, and miR149-5p groups revealed a significant reduction in neurological severity scores following the administration of LV-miR149 and miR149-5p. Each column represents Mean ± SEM ($n = 10$). *$p < 0.05$, **$p < 0.01$, ***$p < 0.001$. MCAO, middle cerebral artery occlusion; LV, lentiviral; miR, microRNA

LV-miR149 group, particularly in the cortex (194.5 ± 23.24 vs. 64.81 ± 9.09) ($p < 0.001$), striatum (60.72 ± 5.61 vs. 39.25 ± 4.57) ($p < 0.05$), and piriform cortex-amygdala (121.1 ± 6 vs. 57.75 ± 20.05) ($p < 0.01$) regions, as well as in the miR149-5p mimic group ((194.5 ± 23.24 vs. 116.8 ± 17.64) $p < 0.05$, (60.72 ± 5.61 vs. 40.48 ± 3.63) $p < 0.05$, and (121.1 ± 6 vs. 68.61 ± 7.27) $p < 0.05$, respectively). In contrast, LV-control had no impact on tissue damage (Fig. 3). In the sham group, Cresyl violet staining of the right brain hemispheres revealed normal-looking neuronal cells with distinct nucleoli and distinct cell boundary. Rats undergoing MCAO displayed numerous dark neurons with shrunken nuclei and perikaryons. The MCAO group exhibited a higher percentage of dark neurons in the cortex (27.41 ± 4.83 vs. 5.73 ± 0.98) ($p < 0.01$), striatum (38.45 ± 3.92 vs. 4.63 ± 0.85) ($p < 0.001$), and piriform cortex (41.37 ± 4.18 vs. 7.08 ± 0.92) ($p < 0.001$) compared to the sham group. Treatment with LV-miR149 decreased the percentage of dark neurons in these regions compared to the right hemisphere of the MCAO model group ((11.62 ± 2.85 vs. 27.41 ± 4.83) $p < 0.05$, (14.62 ± 2.71 vs. 38.45 ± 3.92) $p < 0.001$, (15.18 ± 3.07 vs. 41.37 ± 4.18) $p < 0.001$, respectively). Similarly, the miR149-5p mimic group also showed a significant decrease in the percentage of dark neurons in the striatum (16.53 ± 2.95 vs. 38.45 ± 3.92) ($p < 0.001$), and piriform cortex (19.34 ± 2.83 vs. 41.37 ± 4.18) ($p < 0.001$) (Fig. 4).

Preservation of blood-brain Barrier Integrity by miR-149 Administration

Assessment of blood-brain barrier (BBB) permeability using Evans blue concentration as an indicator revealed an increase in Evans blue concentration in the MCAO group compared to the sham group in the cortex (0.33 ± 0.003 vs. 0.06 ± 0.005) ($p < 0.001$), piriform cortex-amygdala (0.59 ± 0.04 vs. 0.20 ± 0.03) ($p < 0.01$), and striatum (1.54 ± 0.06 vs. 0.36 ± 0.05) ($p < 0.001$). The analysis demonstrated a significant reduction in Evans blue concentration in the cortex (0.24 ± 0.02 vs. 0.33 ± 0.003) ($p < 0.001$) and striatum (0.99 ± 0.04 vs. 1.54 ± 0.06) ($p < 0.001$) following the intraventricular injection of miR149-5p mimic

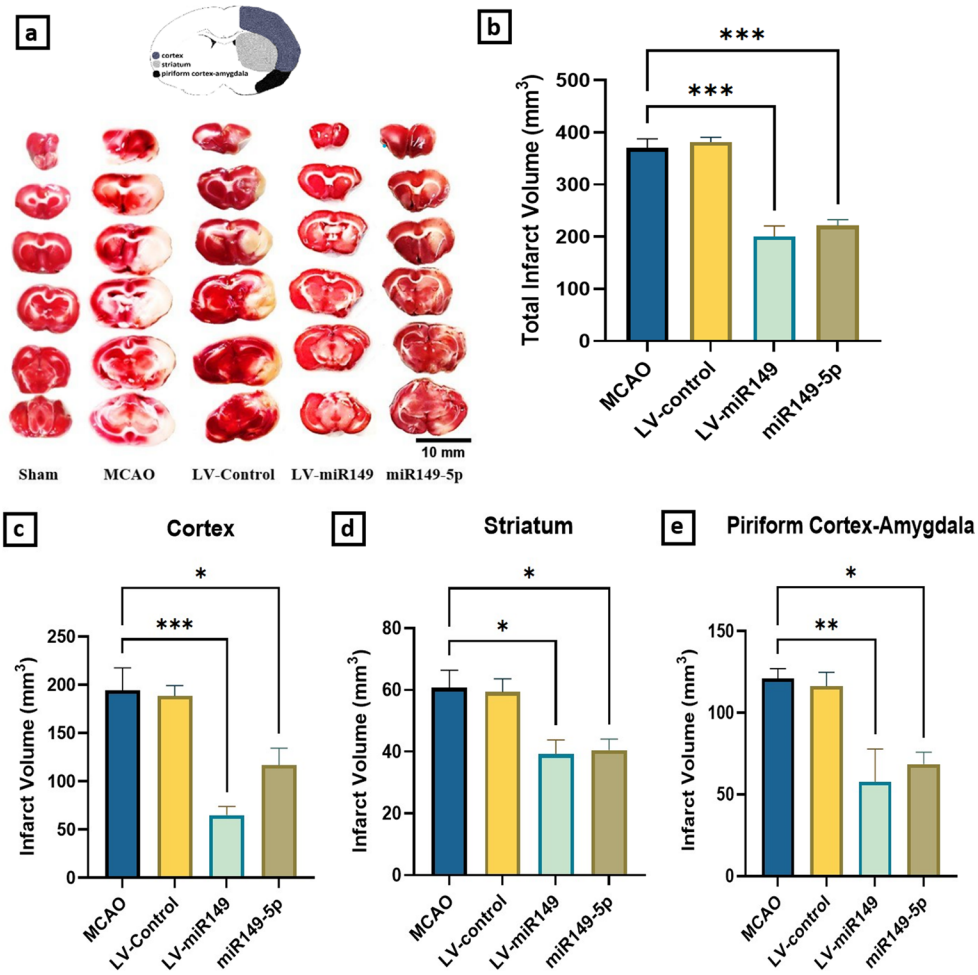

Fig. 3 The effect of miR-149 administration on (**a**) TTC staining of brain tissue slides, (**b**) Total infarct volume, and specific infarct volumes in (**c**) cortex, (**d**) striatum, and (**e**) piriform cortex-amygdala was presented in Sham, MCAO, LV-control, LV-miR149, and miR149-5p groups. MCAO induced severe brain tissue injury in rats, resulting in noticeable neurological deficits in cortical and subcortical regions. Treatment with LV-miR149 and miR149-5p led to a significant reduction in damaged tissue volume. Each column represents Mean ± SEM ($n = 5$). *$p < 0.05$, **$p < 0.01$, ***$p < 0.001$. MCAO, middle cerebral artery occlusion; LV, lentiviral; miR, microRNA

compared to the MCAO group. Similarly, LV-miR149 significantly reduced Evans blue concentration in the cortex (0.12 ± 0.004 vs. 0.33 ± 0.003) ($p < 0.001$), piriform cortex-amygdala (0.30 ± 0.08 vs. 0.59 ± 0.04) ($p < 0.05$), and striatum (0.76 ± 0.03 vs. 1.54 ± 0.06) ($p < 0.001$) compared to the MCAO group. These findings suggest an enhanced integrity of the blood-brain barrier in these treatment groups (Fig. 5).

Attenuation of Cerebral Edema Following miR-149 Treatment

Cerebral ischemia caused by the MCAO method resulted in elevated brain water content in the damaged hemisphere. Notably, treatment with LV-miR149 significantly reduced brain water content in the cortex (80.29 ± 1.1 vs. 86.67 ± 0.94) ($p < 0.01$), striatum (77.33 ± 2.31 vs. 85.37 ± 0.57) ($p < 0.01$), and piriform cortex-amygdala (79.73 ± 1.29 vs. 85.58 ± 0.77) ($p < 0.05$) compared to the right hemisphere of the MCAO model group. Similarly, in the miR149-5p mimic group, a significant reduction in brain water content was observed in the cortex (80.46 ± 1.35 vs. 86.67 ± 0.94) ($p < 0.01$), striatum (77.60 ± 0.87 vs. 85.37 ± 0.57) ($p < 0.01$), and piriform cortex-amygdala (79.83 ± 1.30 vs. 85.58 ± 0.77) ($p < 0.05$) compared to the right hemisphere of the MCAO model group (Fig. 6).

Real-Time PCR

Expression levels of miR149-5p (Fig. 7a), Faslg (Fig. 7b), and GRIN1 (Fig. 7c) were assessed within the cortex, striatum, and piriform cortex-amygdala regions of rats. In comparison to sham-operated rats, MCAO rats exhibited decreased miR149-5p levels, which were subsequently elevated through treatment with LV-miR149 or miR149-5p mimic. Conversely, the expression levels of Faslg and GRIN1 were heightened in MCAO rats but attenuated with LV-miR149 or miR149-5p mimic intervention. Notably, the LV-miR149 treatment significantly reduced Faslg expression levels in the cortex (0.67 ± 0.07 vs. 1.57 ± 0.17) ($p < 0.01$), striatum (0.59 ± 0.15 vs. 85.58 ± 0.77) ($p < 0.01$), and piriform cortex-amygdala (0.59 ± 0.14 vs. 2.96 ± 0.62) ($p < 0.01$) compared to the MCAO model group's right hemisphere. Similarly, this treatment significantly decreased

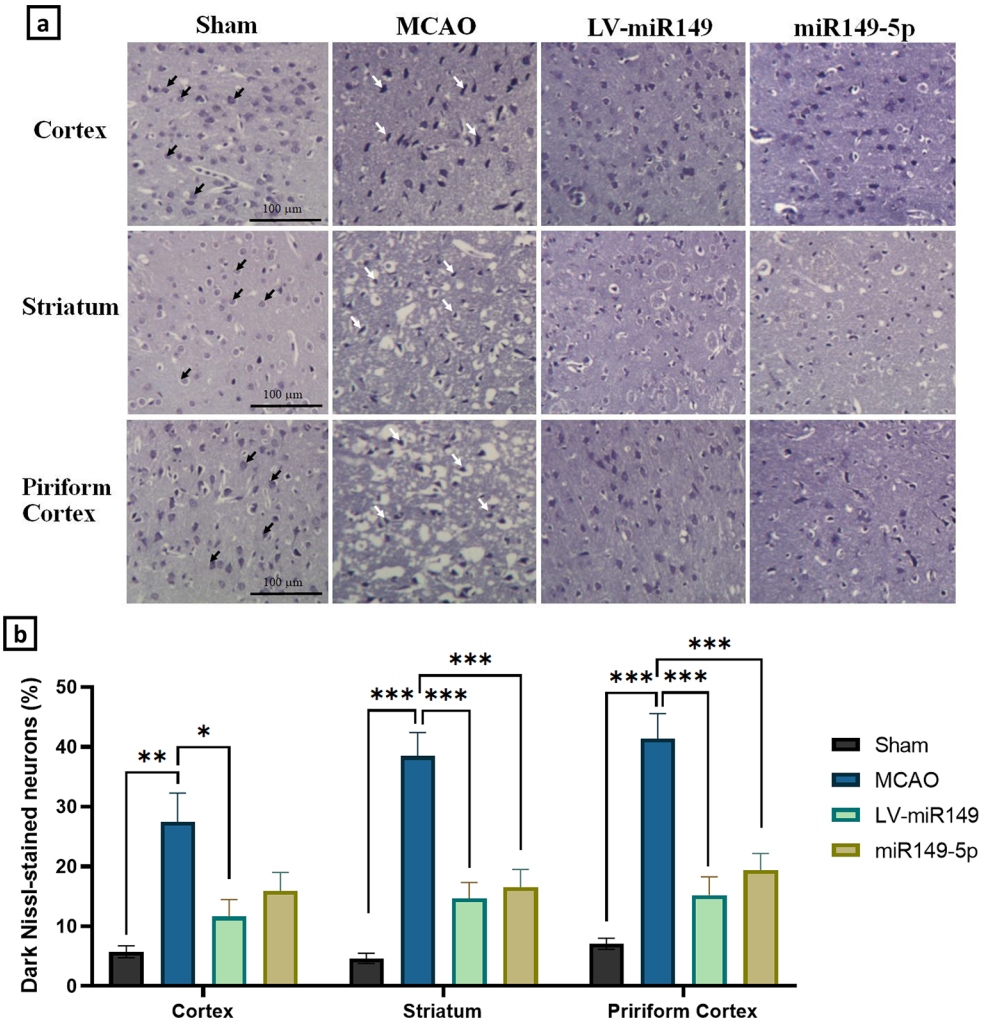

Fig. 4 The effect of miR-149 administration on dark neurons in Nissl-stained sections of the cortex, striatum, and piriform cortex was investigated in Sham, MCAO, LV-miR149, and miR149-5p groups (**a**, **b**). Cresyl violet staining revealed neurodegeneration in the MCAO group, while treatment with LV-miR149 and miR149-5p significantly reduced neurodegeneration. Black arrows show survived neurons, and white arrows indicate pyknotic and dead neurons. Each column represents Mean ± SEM ($n = 5$). *$p < 0.05$, **$p < 0.01$, ***$p < 0.001$. MCAO, middle cerebral artery occlusion; LV, lentiviral; miR, microRNA

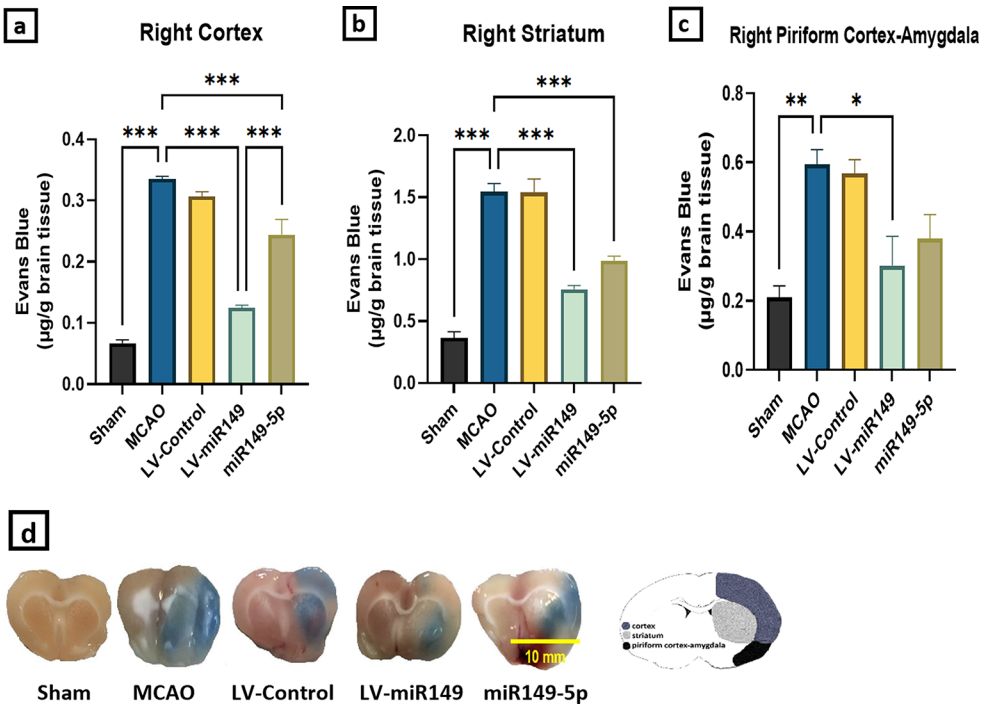

Fig. 5 The effect of miR-149 administration on Evans blue concentration in (**a**) cortex, (**b**) striatum, and (**c**) piriform cortex-amygdala, along with (**d**) Brain Image, was evaluated in Sham, MCAO, LV-control, LV-miR149, and miR149-5p groups. The study assessed the changes in Evans blue concentration as an indicator of blood-brain barrier permeability, reflecting the impact of stroke and the therapeutic intervention with LV-miR149 and miR149-5p on reducing permeability. Each column represents Mean ± SEM ($n = 5$). *$p < 0.05$, **$p < 0.01$, ***$p < 0.001$. MCAO, middle cerebral artery occlusion; LV, lentiviral; miR, microRNA

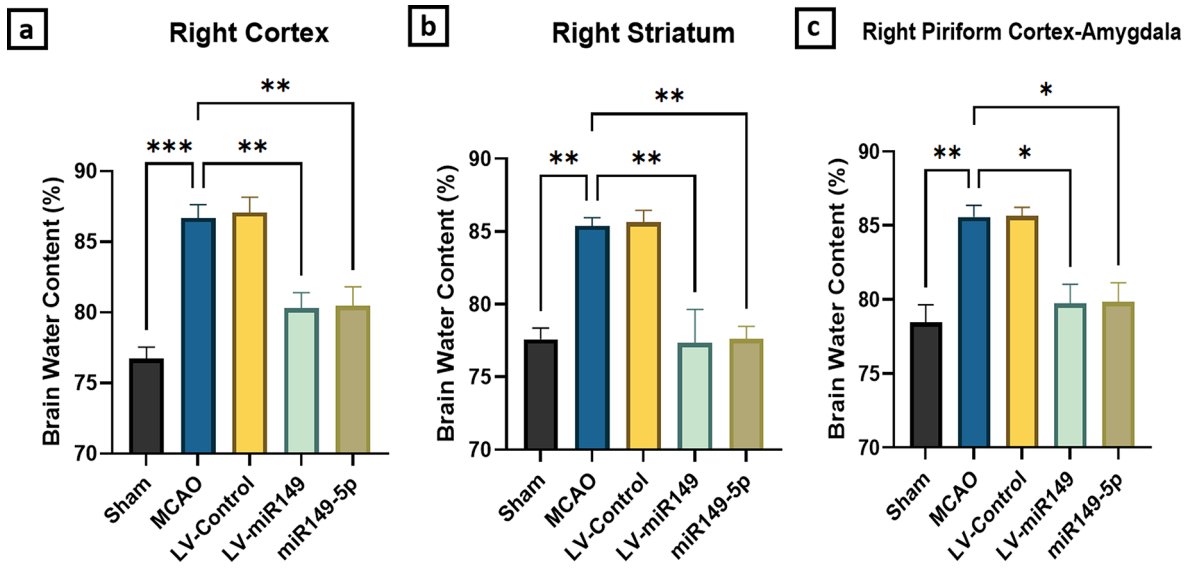

Fig. 6 The effect of miR-149 administration on cerebral edema in (**a**) cortex, (**b**) striatum, and (**c**) piriform cortex-amygdala was assessed in Sham, MCAO, LV-control, LV-miR149, and miR149-5p groups. The study investigated the impact of MCAO-induced cerebral edema and evaluated the therapeutic potential of LV-miR149 and miR149-5p in reducing this edema. Each column represents Mean ± SEM ($n = 5$). *$p < 0.05$, **$p < 0.01$, ***$p < 0.001$. MCAO, middle cerebral artery occlusion; LV, lentiviral; miR, microRNA

GRIN1 expression levels in the cortex (0.37 ± 0.11 vs. 1.004 ± 0.13) ($p < 0.05$), striatum (0.5 ± 0.06 vs. 1.33 ± 0.19) ($p < 0.01$), and piriform cortex-amygdala (0.87 ± 0.17 vs. 2.51 ± 0.32) ($p < 0.05$).

Effect of LV-miR149 on Oxidant and Antioxidant Parameters

We examined the parameters associated with oxidative stress in the ischemic regions, including the cortex, striatum, and piriform cortex-amygdala. The MCAO group exhibited a significant increase in nitrite and MDA levels compared to the sham group in all three regions. However, the injection of LV-miR149 resulted in a significant reduction in nitrite levels in the cortex (0.64 ± 0.02 vs. 1.27 ± 0.14 $p < 0.05$), striatum (1.39 ± 0.09 vs. 2.08 ± 0.19 $p < 0.05$), and piriform cortex-amygdala (0.85 ± 0.07 vs. 1.24 ± 0.04 $p < 0.01$), compared to the MCAO group (Fig. 8a). Additionally, treatment with LV-miR149 led to a significant decrease in MDA levels in the cortex (1.02 ± 0.04 vs. 1.32 ± 0.05 $p < 0.05$) and piriform cortex-amygdala (0.80 ± 0.04 vs. 1.35 ± 0.05 $p < 0.001$) (Fig. 8b).

There were significant decreases in the levels of SOD (Fig. 9a), CAT (Fig. 9b), GSH (Fig. 10a), GPx (Fig. 10b), and GR (Fig. 10c) in the MCAO group compared to the sham group in the cortex, striatum, and piriform cortex-amygdala. However, the upregulation of miR149 led to increased levels of these factors in the ischemic regions. Notably, LV-miR149 treatment significantly increased SOD levels in the cortex (21.82 ± 0.52 vs. 15.67 ± 1.15) ($p < 0.001$), striatum (50.78 ± 3.39 vs. 33.95 ± 1.3) ($p < 0.01$), and piriform cortex-amygdala (27.33 ± 0.82 vs. 20.78 ± 1.81) ($p < 0.01$) compared to the MCAO model group's right hemisphere. Similarly, this treatment notably elevated CAT levels in the cortex (7.61 ± 0.72 vs. 4.6 ± 0.45) ($p < 0.01$), striatum (14.01 ± 1.18 vs. 10.27 ± 0.49) ($p < 0.05$), and piriform cortex-amygdala (10.34 ± 0.45 vs. 6.58 ± 0.37) ($p < 0.01$). Additionally, significant increases were observed in GSH levels in the cortex (276.7 ± 24.19 vs. 133.5 ± 9.19) ($p < 0.01$), striatum (443.5 ± 46.04 vs. 281.7 ± 20.07) ($p < 0.05$), and piriform cortex-amygdala (282.6 ± 8.57 vs. 167.1 ± 15.72) ($p < 0.05$), as well as in GPx levels in the cortex (367.5 ± 40.57 vs. 214.2 ± 18.2) ($p < 0.01$), striatum (794.8 ± 51.63 vs. 491.5 ± 32.41) ($p < 0.01$), and piriform cortex-amygdala (399.6 ± 15.89 vs. 293.5 ± 13.13) ($p < 0.05$). Likewise, there were significant enhancements in GR levels in the cortex (71.50 ± 5.46 vs. 34.96 ± 9.93) ($p < 0.05$), striatum (61.71 ± 4.05 vs. 43.51 ± 4.48) ($p < 0.05$), and piriform cortex-amygdala (72.61 ± 7.82 vs. 36.25 ± 3.98) ($p < 0.01$).

Effect of LV-miR149 on Caspases 1 and 3 and DNA Fragmentation

In the ischemic brain regions, caspase-1 activity significantly increased in the MCAO group compared to the sham group in the cortex (0.154 ± 0.01 vs. 0.079 ± 0.006) ($p < 0.01$), striatum (0.081 ± 0.005 vs. 0.057 ± 0.001) ($p < 0.001$), and piriform cortex-amygdala (0.099 ± 0.004 vs. 0.067 ± 0.002) ($p < 0.001$). However, the LV-miR149

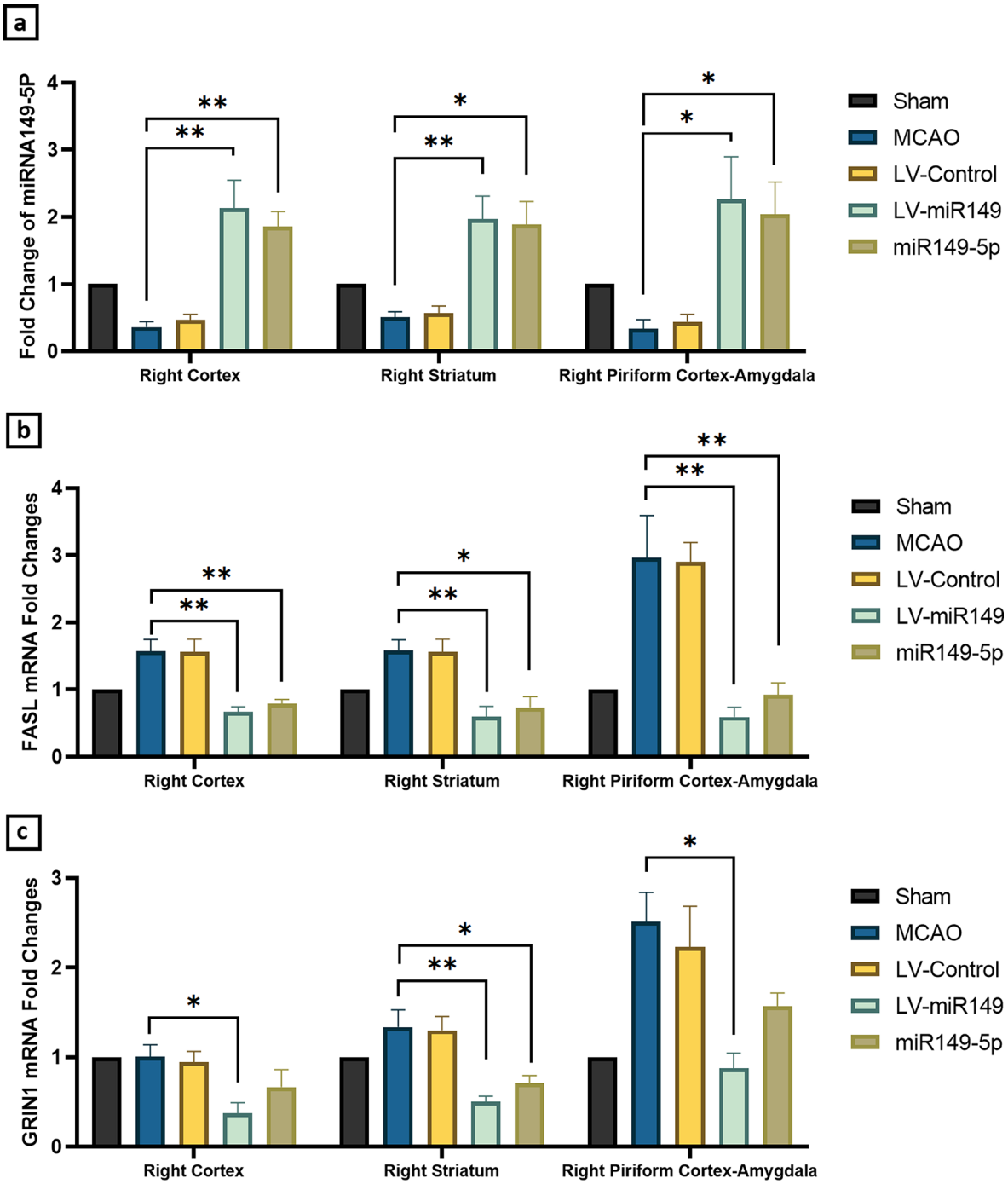

Fig. 7 The effect of miR-149 administration on the expression levels of miR149-5p (**a**), Fas ligand (FASL) (**b**), and Glutamate Receptor Ionotropic NMDA 1(GRIN1) (**c**) was assessed in Sham, MCAO, LV-control, LV-miR149, and miR149-5p groups. The results revealed a decrease in miR149-5p levels and an increase in FASL and GRIN1 levels in the MCAO group, while an increase in miR149-5p levels and a decrease in FASL and GRIN1 levels were observed in the LV-miR149 and miR149-5p treatment groups. Each column represents Mean ± SEM ($n = 3$). *$p < 0.05$, **$p < 0.01$. MCAO, middle cerebral artery occlusion; LV, lentiviral; miR, microRNA

group exhibited a significant decrease ($p < 0.01$) in caspase-1 activity in the cortex (0.083 ± 0.006 vs. 0.154 ± 0.01), striatum (0.063 ± 0.003 vs. 0.081 ± 0.005), and piriform cortex-amygdala (0.074 ± 0.005 vs. 0.099 ± 0.004) regions compared to the MCAO group (Fig. 11a). Similarly, caspase-3 activity in the ischemic brain regions significantly increased in the MCAO group compared to the sham group in the cortex (0.12 ± 0.007 vs. 0.09 ± 0.007) ($p < 0.05$) and piriform cortex-amygdala (0.09 ± 0.01 vs. 0.07 ± 0.001) ($p < 0.05$). Additionally, in the LV-miR149 group, there

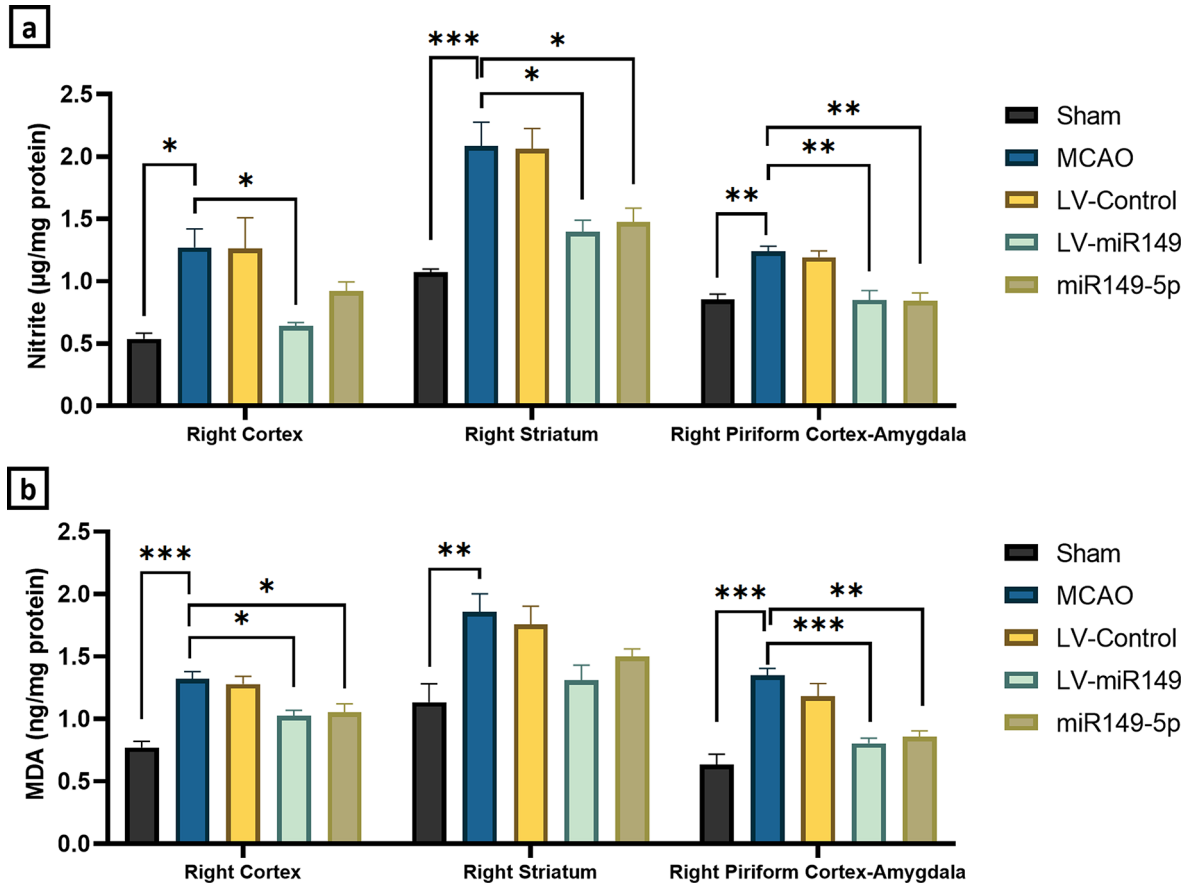

Fig. 8 The effect of miR-149 administration on the levels of oxidative stress parameters: (**a**) nitrite and (**b**) malondialdehyde (MDA) in Sham, MCAO, LV-control, LV-miR149, and miR149-5p groups. The results indicated an increase in nitrite and malondialdehyde levels in the MCAO group and a decrease in the LV-miR149 and miR149-5p treatment groups. Each column represents Mean ± SEM ($n = 4$). *$p < 0.05$, **$p < 0.01$, ***$p < 0.001$. MCAO, middle cerebral artery occlusion; LV, lentiviral; miR, microRNA

was a significant decrease ($p < 0.05$) in caspase-3 activity in the cortex (0.09 ± 0.005 vs. 0.12 ± 0.007) and piriform cortex-amygdala (0.07 ± 0.001 vs. 0.09 ± 0.01) regions compared to the MCAO group. In the striatum, no significant differences were observed for caspase-3 activity within the groups, and therefore, the results for this region were excluded from the analysis (Fig. 11b). Statistical analysis of apoptosis-associated data indicated significant differences between the groups for DNA fragmentation. In the ischemic regions of the brain, DNA fragmentation significantly increased in the MCAO group compared to the sham group ($p < 0.01$) in the cortex (0.88 ± 0.058 vs. 0.45 ± 0.058), striatum (0.97 ± 0.091 vs. 0.46 ± 0.073), and piriform cortex-amygdala (0.85 ± 0.056 vs. 0.35 ± 0.049). However, the LV-miR149 group showed a significant decrease in DNA fragmentation in the cortex (0.58 ± 0.1 vs. 0.88 ± 0.058) ($p < 0.05$), striatum (0.55 ± 0.064 vs. 0.97 ± 0.091) ($p < 0.01$), and piriform cortex-amygdala (0.44 ± 0.085 vs. 0.85 ± 0.056) ($p < 0.05$) regions compared to the MCAO group (Fig. 11c).

Effect of LV-miR149 Treatment on Inflammatory Factors

In this study, we assessed the inflammatory effects by measuring the levels of TNF-α and IL-17 as pro-inflammatory factors and IL-10 as an anti-inflammatory factor. The MCAO group showed a significant increase in TNF-α (Fig. 12a) ((276.7 ± 10.67 to 169.4 ± 11.14) $p < 0.001$, (753.7 ± 51.35 to 469.4 ± 25.88) $p < 0.01$, and (362.3 ± 11.37 to 212.9 ± 9.226) $p < 0.001$, respectively) and IL-17 ((159.6 ± 6.91 to 92.16 ± 8.22) $p < 0.001$, (435.8 ± 15.29 to 243.3 ± 10.68) $p < 0.001$, and (189.0 ± 7.69 to 125.6 ± 13.56) $p < 0.001$, respectively) (Fig. 12b) levels in the cortex, striatum, and piriform cortex-amygdala areas compared to the sham group. Additionally, the level of IL-10 (Fig. 12c) was increased in the MCAO group. In the group treated with LV-miR149, we observed a decrease in the levels of IL-17 ((102.2 ± 8.62 to 159.6 ± 6.91) $p < 0.01$, (294.4 ± 23.34 to 435.8 ± 15.29) $p < 0.01$, and (141.7 ± 6.5 to 189.0 ± 7.69) $p < 0.05$, respectively) and TNF-α ((184.5 ± 15.59 to 276.7 ± 10.67) $p < 0.01$, (523.6 ± 27.44 to 753.7 ± 51.35)

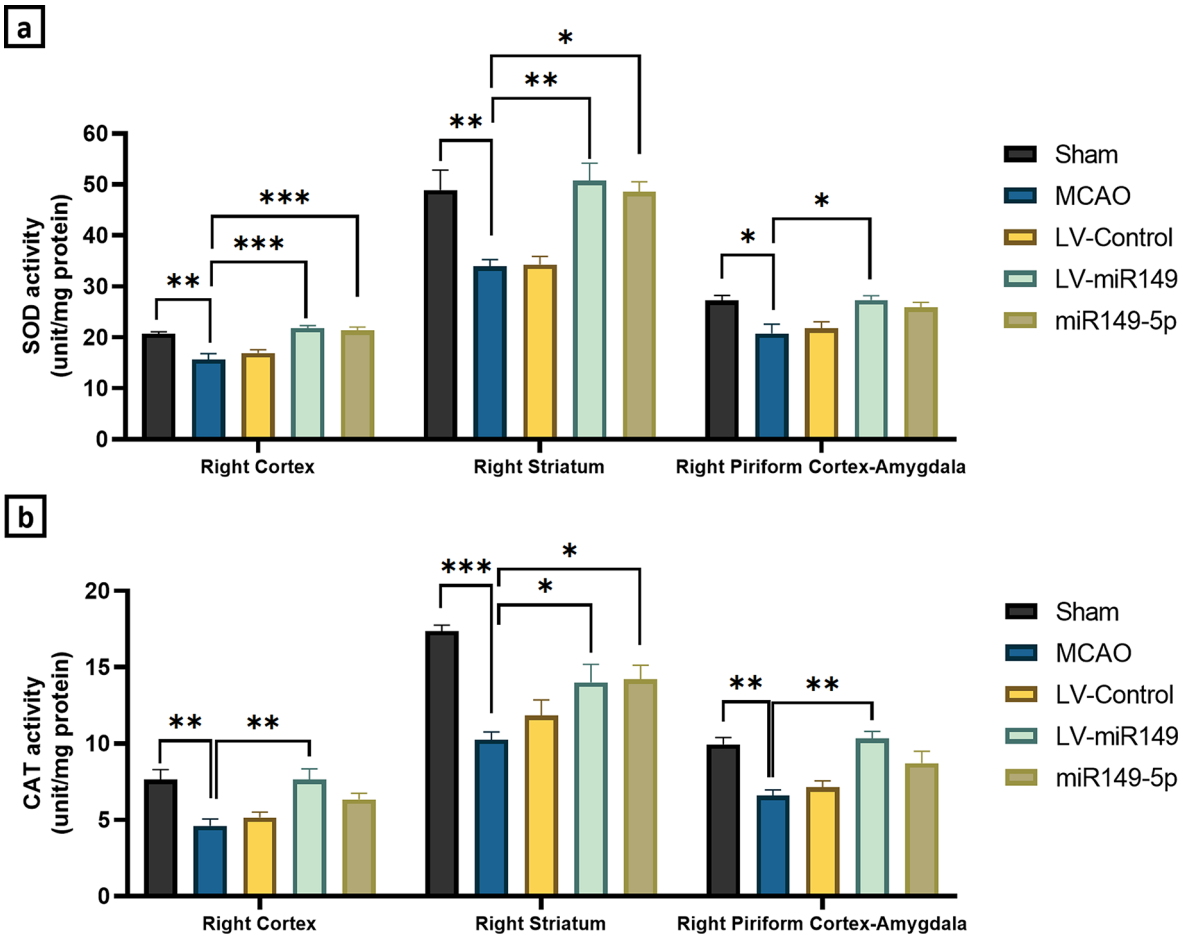

Fig. 9 The effect of miR-149 administration on the levels of antioxidant parameters: (**a**) superoxide dismutase (SOD), (**b**) catalase (CAT) in Sham, MCAO, LV-control, LV-miR149, and miR149-5p groups. Results revealed a decrease in SOD and CAT levels in the MCAO group, indicative of oxidative stress. Conversely, treatment with LV-miR149 and miR149-5p shows a significant increase in SOD and CAT levels, suggesting a potential therapeutic effect in mitigating oxidative stress. Each column represents Mean ± SEM ($n = 4$). *$p < 0.05$, **$p < 0.01$, ***$p < 0.001$. MCAO, middle cerebral artery occlusion; LV, lentiviral; miR, microRNA

$p < 0.01$, and (282.3 ± 15.88 to 362.3 ± 11.37) $p < 0.01$, respectively) compared to the ischemic group. Furthermore, while the increase in IL-10 did not reach statistical significance compared to the MCAO group, it was significantly higher than the sham group in all three investigated areas ((216.5 ± 22.23 to 121.7 ± 9.79) $p < 0.01$, (650.4 ± 63.79 to 396.0 ± 11.20) $p < 0.05$, and (271.2 ± 22.75 to 157.3 ± 16.40) $p < 0.01$, respectively).

Discussion

This study aimed to assess how miR-149 influences neurological deficits in ischemic stroke. Employing the MCAO model to generate focal cerebral ischemia phenotype, we noted a substantial reduction in neurological deficit scores, BBB permeability, and stroke volume with increased miR-149 expression. Additionally, markers of oxidative stress, inflammation, and cell death exhibited a decline in the treatment group.

Ischemic stroke induces behavioral dysfunction and neuronal injury in distinct brain regions, leading to neurobehavioral disorders [28, 29], as observed in this study. This study underscores the need for targeted therapeutic interventions addressing specific brain areas to optimize treatment for neurobehavioral disorders resulting from ischemic stroke. Also, ischemic stroke disrupts the blood-brain barrier (BBB), causing persistent permeability. Matrix metalloproteinases (MMPs), including MMP-2 and MMP-9, initiate BBB breakdown. Therapies targeting these factors aim to preserve the BBB [30]. Consistent with the findings of this study, earlier research has demonstrated decreased miR149-5p expression in cerebral ischemia cases [31]. Moreover, miR-149 mimic led to reduced matrix metalloproteinase (MMP) levels, significantly lowering blood-brain barrier (BBB) permeability. This outcome was linked to improved

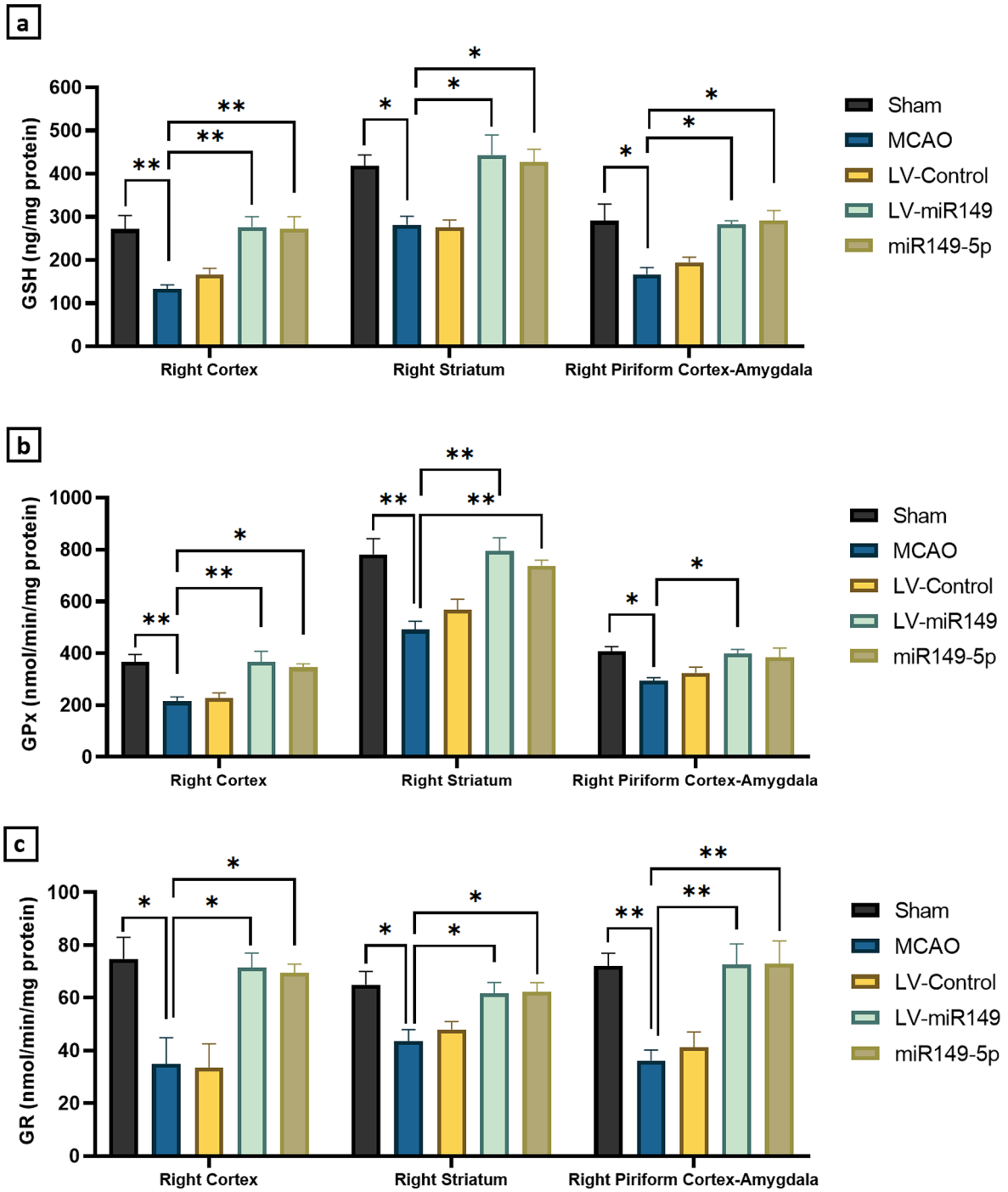

Fig. 10 The effect of miR-149 administration on the levels of antioxidant parameters: (**a**) glutathione (GSH), (**b**) glutathione peroxidase (GPx), and (**c**) glutathione reductase (GR) in Sham, MCAO, LV-control, LV-miR149, and miR149-5p groups. Results show alterations in antioxidant parameters, revealing a decrease in GSH, GPx, and GR levels in the MCAO group, indicative of oxidative stress. Conversely, treatment with LV-miR149 and miR149-5p demonstrates a significant increase in GSH, GPx, and GR levels, suggesting a potential therapeutic effect in alleviating oxidative stress. Each column represents Mean ± SEM ($n = 4$). *$p < 0.05$, **$p < 0.01$. MCAO, middle cerebral artery occlusion; LV, lentiviral; miR, microRNA

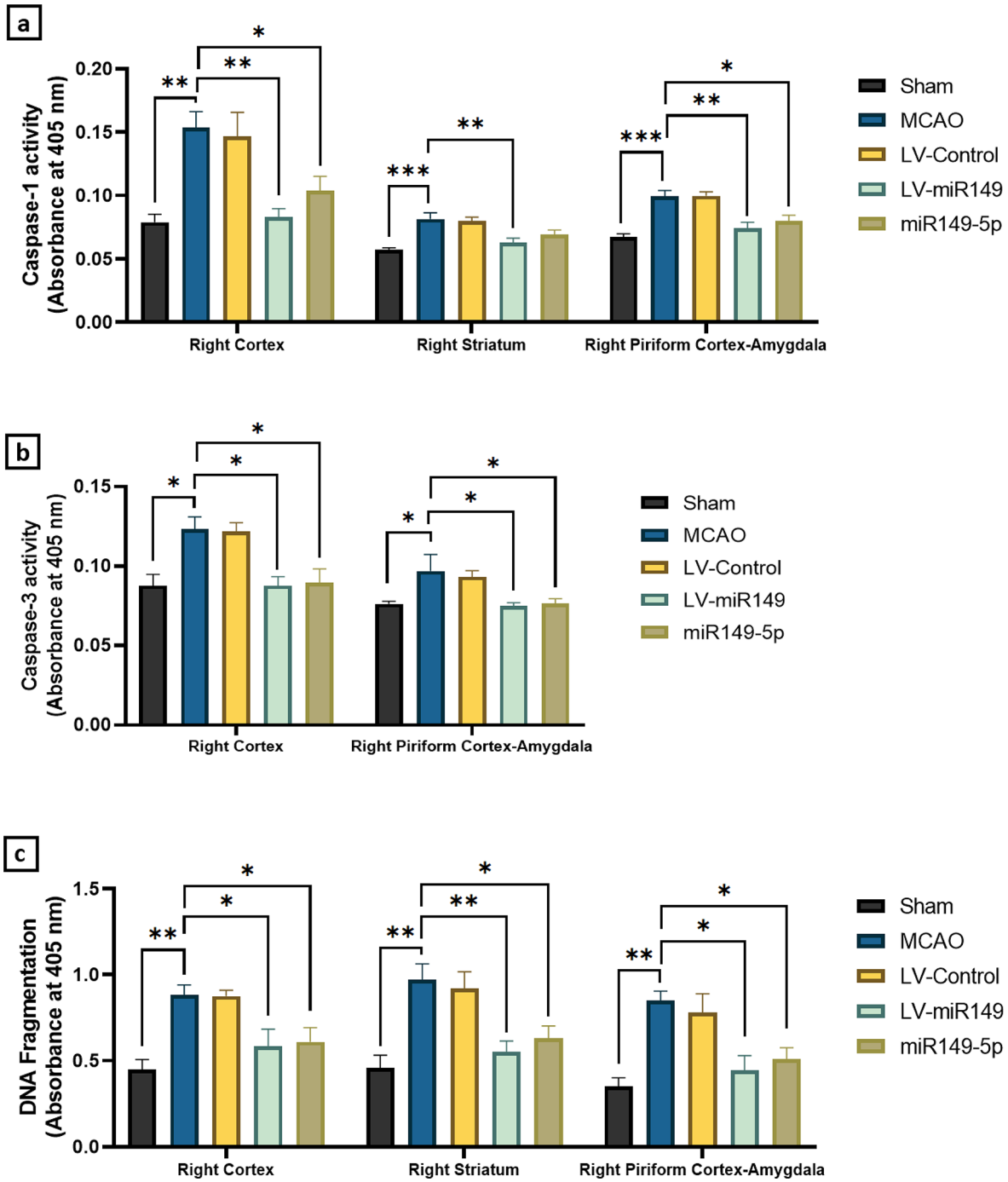

Fig. 11 The effect of miR-149 administration on the levels of caspase-1 (**a**), caspase-3 (**b**), and changes in DNA fragmentation (**c**) was evaluated in Sham, MCAO, LV-control, LV-miR149, and miR149-5p groups. Results indicated alterations in caspase-1 and −3 activity levels, and DNA fragmentation, suggesting an increase in the MCAO group, indicative of apoptotic and pyroptotic processes. Conversely, treatment with LV-miR149 and miR149-5p demonstrated a significant decrease in caspase-1 and −3 activity levels, and DNA fragmentation, implying potential anti-apoptotic and anti-pyroptotic effects. Each column represents Mean ± SEM ($n = 4$). *$p < 0.05$, **$p < 0.01$, ***$p < 0.001$. MCAO, middle cerebral artery occlusion; LV, lentiviral; miR, microRNA

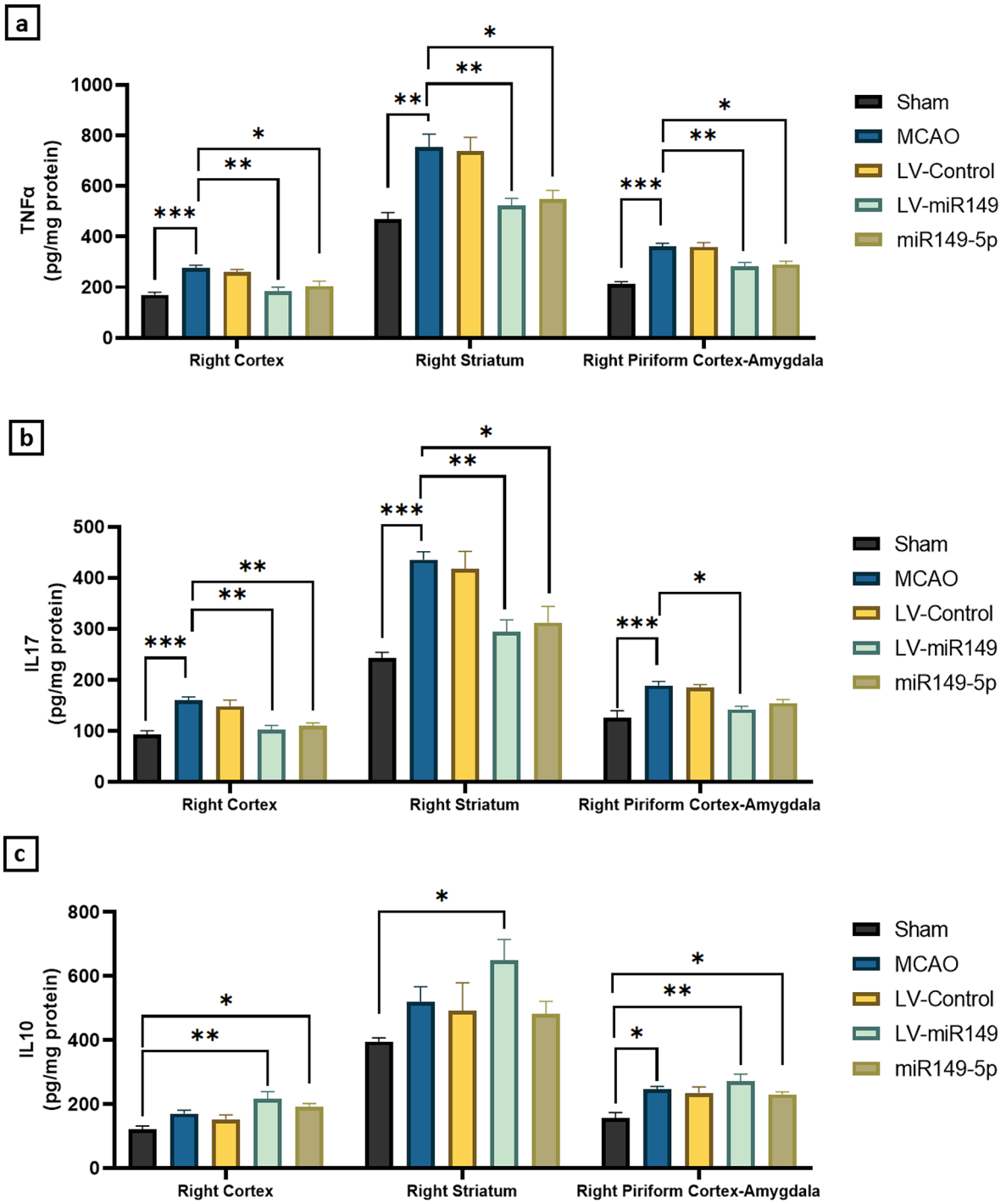

Fig. 12 The effect of miR-149 administration on the levels of the inflammatory and anti-inflammatory factors: (**a**) tumor necrosis factor-α (TNF-α), (**b**) interleukin-17 (IL-17), and (**c**) interleukin-10 (IL-10) in Sham, MCAO, LV-control, LV-miR149, and miR149-5p groups. Findings revealed variations in these factors, showcasing an increase in TNF-α and IL-17 levels and a decrease in IL-10 levels in the MCAO group, suggesting an inflammatory response. Conversely, treatment with LV-miR149 and miR149-5p significant reduced TNF-α and IL-17 levels and an increase in IL-10 levels, indicating a potential anti-inflammatory effect. Each column represents Mean ± SEM ($n = 4$). *$p < 0.05$, **$p < 0.01$, ***$p < 0.001$. MCAO, middle cerebral artery occlusion; LV, lentiviral; miR, microRNA

expression of tight junction proteins and increased pericyte coverage, as reported before [12].

Oxidative stress plays a critical role in stroke pathophysiology, leading to cellular damage and exacerbating brain injury. In our study, miR-149 increase demonstrated promising effects in reducing oxidative stress by enhancing endogenous antioxidant defenses, including GSH, SOD, CAT, GPx, and GR, during ischemia-reperfusion injury. According to previous research, these antioxidants contribute to the cell's overall antioxidant capacity, providing vital defense against oxidative stress. Specifically, SOD converts superoxide radicals into hydrogen peroxide, which is converted into oxygen and water by CAT, while GPx utilizes GSH to effectively reduced hydrogen peroxide [32–34]. On the other hand, we observed that malondialdehyde, a biomarker of oxidative stress and cellular toxicity, decreases in response to increased levels of miR-149. Moreover, the upregulation of miR-149 caused a reduction in nitrite levels, which may contribute to decreased blood-brain barrier permeability and brain edema in the treatment group. These findings propose that miR-149's protective effect is via mitigating oxidative stress and neurotoxicity, thus ameliorating BBB integrity and reducing brain edema.

Furthermore, our study focused on post-ischemic inflammation and its impact on secondary brain injury in stroke. By investigating the effects of the miR-149 on inflammation, we measured the levels of pro-inflammatory cytokines (TNF-α and IL-17) and an anti-inflammatory cytokine (IL-10) in the MCAO model. The results showed that increased miR-149 expression caused the suppression of pro-inflammatory cytokines in the MCAO model. Previous studies have also displayed that miR-149 has an anti-inflammatory role. Qin et al. demonstrated its efficacy by targeting IL-6 and TNF-α mRNAs [13]. In liver inflammation, miR-149 acts as a suppressor by targeting STAT3 [35]. In osteoarthritis, miR-149 reduces inflammation through VCAM-1 (Vascular Cell Adhesion Molecule-1) and phosphoinositide 3-kinase (PI3K)/AKT inhibition [36]. It downregulates IL-1α, IL-1β, and IL-6, demonstrating its positive role in inflammation reduction [37]. In myocardial I/R damage, miR-149 targets forkhead box O3 (FoxO3), influencing pyroptosis and inflammation [38]. These effects suggest its potential as an agent to mitigate the neuroinflammatory cascade and promote tissue repair.

Cell death significantly contributes to neuronal loss in the ischemic penumbra following stroke. Our study focused on assessing the impact of the miR-149 on cell death by examining some of its key markers involved in pyroptosis and apoptosis pathways, including Faslg, GRIN1, caspase-1, -3, and DNA fragmentation. The findings revealed that increased miR-149 expression influences the signaling pathways associated with cell death in the MCAO model. By targeting specific molecules involved in cell death cascades, miR-149 exhibited potential neuroprotective effects, promoting cell survival and limiting cell death. These results align with previous research highlighting miR-149's role as a regulator of apoptotic processes in various cellular contexts [39]. Studies on cancer cells have demonstrated that blocking miR149-5p can lead to an upregulation of FASLG (Fas Ligand), inducing apoptosis by activating FADD (Fas Associated Via Death Domain) and caspases. However, the dual role of miR149-5p in cancer, alternating between an oncogene and an anti-oncogene, is context-dependent and varies based on the specific tumor type. Consequently, further investigations are required to understand its role in this context [40].

Previous studies have shown that ischemic stroke activates caspase-1, resulting in pyroptotic cell death and inflammation [41, 42]. In line with this, our study demonstrated elevated caspase-1 levels 24 h after inducing ischemia, while the mir-149 treatment groups exhibited a significant decrease. On the other hand, cerebral ischemia involves both intrinsic and extrinsic apoptosis pathways. The intrinsic pathways include damaged mitochondria, cytochrome c release, and caspase-3 activation, leading to DNA cleavage and neuronal apoptosis. Activation of death receptors in the extrinsic pathway leads to mitochondrial membrane permeability, DNA cleavage, and apoptosis. Caspase-3 cleaves substrates, inducing apoptotic cell death and energy depletion. Targeting caspase-3 or death receptors reduces post-MCAO cerebral infarct volume [43, 44]. Published evidence links caspase-3 to cerebrovascular injuries and its increase is observed in various neurological conditions [45, 46]. Thus, we measured caspase-3 and DNA fragmentation levels in this study, confirming reduced caspase-3 levels in miR-149-treated groups, suggesting potential neuroprotective agents for acute neurodegenerative conditions.

In this study, we focused on the impact of miR-149 on some parameters related to ischemic stroke. Further molecular mechanisms and signaling pathways by which miR-149 acts necessitate additional investigation. Also, a detailed assessment of vascular smooth muscle cell changes in response to MCAO and miR-149 needs further analysis. Because of our limitations, we did not assess apoptotic factors like Bax, Bcl2, and Annexin V, which should be considered in future research. Histochemical assessment of edema is another limitation that needs to be addressed in future investigations.

Conclusion

In summary, our study revealed the neuroprotective potential of miR-149 in ischemic stroke. LV-miR149 or miR149-5p mimic treatment improved neurological function, reduced histopathological changes, preserved BBB integrity, and mitigated cerebral edema, altered expression of miR149-5p, Faslg, and GRIN1, reduced oxidative stress and inflammation, and caspase-1 and −3 activity which well suggests miR-149's therapeutic potential in ischemic stroke.

Acknowledgements No acknowledgments.

Author Contribution The study's conception and design were developed by M.R.B. and M.R., with H.S. and S.A. providing support in procuring necessary equipment. S.V. carried out the experiments, analyzed the data, and drafted the initial manuscript. The culmination of the manuscript was a collaborative effort, with all authors contributing equally to its refinement.

Funding This study received support from a grant (No. 99025398) provided by the Iran National Science Foundation (INSF).

Data Availability Data will be made available on request.

Declarations

Ethics Approval The animal experiments adhered to the National Institute of Health Guide for the Care and Use of Laboratory Animals. The study protocol received approval from the Research Ethics Committees of Shahid Beheshti University (IR.SBU.REC.1400.100), ensuring compliance with ethical standards in research involving laboratory animals.

Consent to Participate Not Applicable.

Consent for Publication Not Applicable.

Competing Interests The authors declare no competing interests.

References

1. Kuriakose D, Xiao Z (Oct. 2020) Pathophysiology and treatment of stroke: Present Status and Future perspectives. Int J Mol Sci 21(20):7609. https://doi.org/10.3390/ijms21207609
2. An SJ, Kim TJ, Yoon B-W (Jan. 2017) Epidemiology, risk factors, and clinical features of Intracerebral Hemorrhage: an update. J Stroke 19(1):3–10. https://doi.org/10.5853/jos.2016.00864
3. Migdady I, Russman A, Buletko AB (2021) Atrial Fibrillation and Ischemic Stroke: A Clinical Review, *Semin. Neurol*, vol. 41, no. 4, pp. 348–364, Aug. https://doi.org/10.1055/s-0041-1726332
4. Wajngarten M, Silva GS (Jul. 2019) Hypertension and stroke: update on treatment. Eur Cardiol Rev 14(2):111–115. https://doi.org/10.15420/ecr.2019.11.1
5. Bulygin KV et al (2020) Sep., Can miRNAs Be Considered as Diagnostic and Therapeutic Molecules in Ischemic Stroke Pathogenesis?-Current Status, *Int. J. Mol. Sci*, vol. 21, no. 18, p. 6728, https://doi.org/10.3390/ijms21186728
6. Liang Y et al (2018) Inhibition of MiRNA-125b decreases cerebral Ischemia/Reperfusion Injury by Targeting CK2α/NADPH oxidase signaling. Cell Physiol Biochem Int J Exp Cell Physiol Biochem Pharmacol 45(5):1818–1826. https://doi.org/10.1159/000487873
7. Aldous EK et al (2022) Mar., Identification of Novel Circulating miRNAs in Patients with Acute Ischemic Stroke, *Int. J. Mol. Sci*, vol. 23, no. 6, p. 3387, https://doi.org/10.3390/ijms23063387
8. Ren F, Yao Y, Cai X, Cai Y, Su Q, Fang G (2021) MiR-149-5p: An Important miRNA Regulated by Competing Endogenous RNAs in Diverse Human Cancers, *Front. Oncol*, vol. 11, p. 743077, Oct. https://doi.org/10.3389/fonc.2021.743077
9. Ruan D, Liu Y, Wang X, Yang D, Sun Y (2019) miR-149-5p protects against high glucose-induced pancreatic beta cell apoptosis via targeting the BH3-only protein BIM, *Exp. Mol. Pathol*, vol. 110, p. 104279, Oct. https://doi.org/10.1016/j.yexmp.2019.104279
10. Khidr EG et al (Aug. 2023) The potential role of miRNAs in the pathogenesis of cardiovascular diseases - a focus on signaling pathways interplay. Pathol Res Pract 248:154624. https://doi.org/10.1016/j.prp.2023.154624
11. Ghasemloo E, Oryan S, Bigdeli MR, Mostafavi H, Eskandari M (2021) The neuroprotective effect of MicroRNA-149-5p and coenzymeQ10 by reducing levels of inflammatory cytokines and metalloproteinases following focal brain ischemia in rats, *Brain Res. Bull*, vol. 169, pp. 205–213, Apr. https://doi.org/10.1016/j.brainresbull.2021.01.013
12. Wan Y et al (2018) Jun., MicroRNA-149-5p regulates blood-brain barrier permeability after transient middle cerebral artery occlusion in rats by targeting S1PR2 of pericytes, *FASEB J. Off. Publ. Fed. Am. Soc. Exp. Biol*, vol. 32, no. 6, pp. 3133–3148, https://doi.org/10.1096/fj.201701121R
13. Qin C, Lv Y, Zhao H, Yang B, Zhang P (2019) MicroRNA-149 Suppresses Inflammation in Nucleus Pulposus Cells of Intervertebral Discs by Regulating MyD88, *Med. Sci. Monit. Int. Med. J. Exp. Clin. Res*, vol. 25, pp. 4892–4900, Jul. https://doi.org/10.12659/MSM.915858
14. Tiscornia G, Singer O, Verma IM (2006) Production and purification of lentiviral vectors. Nat Protoc 1(1):241–245. https://doi.org/10.1038/nprot.2006.37
15. Longa EZ, Weinstein PR, Carlson S, Cummins R (Jan. 1989) Reversible middle cerebral artery occlusion without craniectomy in rats. Stroke 20(1):84–91. https://doi.org/10.1161/01.str.20.1.84
16. Chen J et al (Apr. 2001) Therapeutic benefit of intravenous administration of bone marrow stromal cells after cerebral ischemia in rats. Stroke 32(4):1005–1011. https://doi.org/10.1161/01.str.32.4.1005
17. Swanson RA, Morton MT, Tsao-Wu G, Savalos RA, Davidson C, Sharp FR (1990) A semiautomated method for measuring brain infarct volume, *J. Cereb. Blood Flow Metab. Off. J. Int. Soc. Cereb. Blood Flow Metab*, vol. 10, no. 2, pp. 290–293, Mar. https://doi.org/10.1038/jcbfm.1990.47
18. Torfeh A, Abdolmaleki Z, Nazarian S, Shirazi Beheshtiha SH (2021) Modafinil-coated nanoparticle increases expressions of brain-derived neurotrophic factor, glial cell line-derived neurotrophic factor and neuronal nuclear protein, and protects against middle cerebral artery occlusion-induced neuron apoptosis in the rat hippocampus, *Anat. Rec. Hoboken NJ 2007*, vol. 304, no. 9, pp. 2032–2043, Sep. https://doi.org/10.1002/ar.24581
19. Asgari Taei A, Dargahi L, Khodabakhsh P, Kadivar M, Farahmandfar M (2022) Hippocampal neuroprotection mediated by secretome of human mesenchymal stem cells against experimental stroke, *CNS Neurosci. Ther*, vol. 28, no. 9, pp. 1425–1438, Sep. https://doi.org/10.1111/cns.13886
20. Fernández-López D et al (Jul. 2012) Blood–brain barrier permeability is increased after Acute Adult Stroke but not neonatal stroke

in the rat. J Neurosci 32:9588–9600. https://doi.org/10.1523/JNEUROSCI.5977-11.2012
21. Yang C et al (Dec. 2021) Neurovascular protection by adropin in experimental ischemic stroke through an endothelial nitric oxide synthase-dependent mechanism. Redox Biol 48:102197. https://doi.org/10.1016/j.redox.2021.102197
22. Alizadeh Makvandi A, Khalili M, Roghani M, Amiri Moghaddam S (2021) Hesperetin ameliorates electroconvulsive therapy-induced memory impairment through regulation of hippocampal BDNF and oxidative stress in a rat model of depression, *J. Chem. Neuroanat*, vol. 117, p. 102001, Nov. https://doi.org/10.1016/j.jchemneu.2021.102001
23. Lee JW, Lee D-H, Park JK, Han JS (2019) Sodium nitrite-derived nitric oxide protects rat testes against ischemia/reperfusion injury. Asian J Androl 21(1):92–97. https://doi.org/10.4103/aja.aja_76_18
24. Silva-Islas CA, Chánez-Cárdenas ME, Barrera-Oviedo D, Ortiz-Plata A, Pedraza-Chaverri J, Maldonado PD (2019) Diallyl Trisulfide Protects Rat Brain Tissue against the Damage Induced by Ischemia-Reperfusion through the Nrf2 Pathway, *Antioxidants*, vol. 8, no. 9, p. 410, Sep. https://doi.org/10.3390/antiox8090410
25. De Meyer SF, Suidan GL, Fuchs TA, Monestier M, Wagner DD (2012) Extracellular chromatin is an important mediator of ischemic stroke in mice, *Arterioscler. Thromb. Vasc. Biol*, vol. 32, no. 8, pp. 1884–1891, Aug. https://doi.org/10.1161/ATVBAHA.112.250993
26. Khaleghi-Mehr M, Delshad A-A, Shafie-Damavandi S, Roghani M (2023) Metformin mitigates amyloid β1-40-induced cognitive decline via attenuation of oxidative/nitrosative stress and neuroinflammation, *Metab. Brain Dis*, vol. 38, no. 4, pp. 1127–1142, Apr. https://doi.org/10.1007/s11011-023-01170-1
27. Albazal A, Delshad A-A, Roghani M (Mar. 2021) Melatonin reverses cognitive deficits in streptozotocin-induced type 1 diabetes in the rat through attenuation of oxidative stress and inflammation. J Chem Neuroanat 112:101902. https://doi.org/10.1016/j.jchemneu.2020.101902
28. Balbinot G, Schuch CP (2019) Compensatory Relearning Following Stroke: Cellular and Plasticity Mechanisms in Rodents, *Front. Neurosci*, vol. 12, Accessed: Nov. 24, 2023. [Online]. Available: https://www.frontiersin.org/articles/https://doi.org/10.3389/fnins.2018.01023
29. Lima RR et al (2016) Neurodegeneration and glial response after Acute Striatal Stroke: histological basis for neuroprotective studies. Oxid Med Cell Longev 2016:3173564. https://doi.org/10.1155/2016/3173564
30. Nian K, Harding IC, Herman IM, Ebong EE (2020) Blood-Brain Barrier Damage in Ischemic Stroke and Its Regulation by Endothelial Mechanotransduction, *Front. Physiol*, vol. 11, Accessed: Dec. 01, 2023. [Online]. Available: https://www.frontiersin.org/articles/https://doi.org/10.3389/fphys.2020.605398
31. Sun P, Hamblin MH, Yin K-J (Mar. 2022) Non-coding RNAs in the regulation of blood–brain barrier functions in central nervous system disorders. Fluids Barriers CNS 19:27. https://doi.org/10.1186/s12987-022-00317-z
32. Kamal FZ, Lefter R, Jaber H, Balmus I-M, Ciobica A, Iordache A-C (2023) The Role of Potential Oxidative Biomarkers in the Prognosis of Acute Ischemic Stroke and the Exploration of Antioxidants as Possible Preventive and Treatment Options, *Int. J. Mol. Sci*, vol. 24, no. 7, p. 6389, Mar. https://doi.org/10.3390/ijms24076389
33. Jelinek M, Jurajda M, Duris K (2021) Oxidative Stress in the Brain: Basic Concepts and Treatment Strategies in Stroke, *Antioxidants*, vol. 10, no. 12, Art. no. 12, Dec. https://doi.org/10.3390/antiox10121886
34. Deng Z et al (2022) Sep., Leonurine Reduces Oxidative Stress and Provides Neuroprotection against Ischemic Injury via Modulating Oxidative and NO/NOS Pathway, *Int. J. Mol. Sci*, vol. 23, no. 17, https://doi.org/10.3390/ijms231710188
35. Zhang Q et al (2017) Jun., MicroRNA-149* suppresses hepatic inflammatory response through antagonizing STAT3 signaling pathway, *Oncotarget*, vol. 8, no. 39, pp. 65397–65406, https://doi.org/10.18632/oncotarget.18541
36. Jiang Y, Zhang L, Tian H (Apr. 2023) MicroRNA-149 improves osteoarthritis via repression of VCAM-1 and inactivation of PI3K/AKT pathway. Exp Gerontol 174:112103. https://doi.org/10.1016/j.exger.2023.112103
37. Lang H et al (Aug. 2017) MicroRNA-149 contributes to scarless wound healing by attenuating inflammatory response. Mol Med Rep 16(2):2156–2162. https://doi.org/10.3892/mmr.2017.6796
38. Lin J, Lin H, Ma C, Dong F, Hu Y, Li H (2019) MiR-149 Aggravates Pyroptosis in Myocardial Ischemia-Reperfusion Damage via Silencing FoxO3, *Med. Sci. Monit. Int. Med. J. Exp. Clin. Res*, vol. 25, pp. 8733–8743, Nov. https://doi.org/10.12659/MSM.918410
39. Wang C et al (2023) Jan., Scutellarin Alleviates Ischemic Brain Injury in the Acute Phase by Affecting the Activity of Neurotransmitters in Neurons, *Molecules*, vol. 28, no. 7, Art. no. 7, https://doi.org/10.3390/molecules28073181
40. He Y, Yu D, Zhu L, Zhong S, Zhao J, Tang J (Jan. 2018) miR-149 in Human Cancer: a systemic review. J Cancer 9(2):375–388. https://doi.org/10.7150/jca.21044
41. Ye X et al (2022) Caspase-1: A Promising Target for Preserving Blood–Brain Barrier Integrity in Acute Stroke, *Front. Mol. Neurosci*, vol. 15, Accessed: Jan. 19, 2024. [Online]. Available: https://www.frontiersin.org/articles/https://doi.org/10.3389/fnmol.2022.856372
42. Liang Y et al (2021) Inhibition of Caspase-1 Ameliorates Ischemia-Associated Blood-Brain Barrier Dysfunction and Integrity by Suppressing Pyroptosis Activation, *Front. Cell. Neurosci*, vol. 14, Accessed: Jan. 19, 2024. [Online]. Available: https://www.frontiersin.org/articles/https://doi.org/10.3389/fncel.2020.540669
43. Mao R, Zong N, Hu Y, Chen Y, Xu Y (2022) Neuronal Death Mechanisms and Therapeutic Strategy in Ischemic Stroke, *Neurosci. Bull*, vol. 38, no. 10, pp. 1229–1247, Oct. https://doi.org/10.1007/s12264-022-00859-0
44. Uzdensky AB (2019) Apoptosis regulation in the penumbra after ischemic stroke: expression of pro- and antiapoptotic proteins, *Apoptosis Int. J. Program. Cell Death*, vol. 24, no. 9–10, pp. 687–702, Oct. https://doi.org/10.1007/s10495-019-01556-6
45. Dailah HG (2022) Potential of Therapeutic Small Molecules in Apoptosis Regulation in the Treatment of Neurodegenerative Diseases: An Updated Review, *Mol. Basel Switz*, vol. 27, no. 21, p. 7207, Oct. https://doi.org/10.3390/molecules27217207
46. Aycan A et al (Jan. 2023) Evaluation of cholinergic enzymes and selected biochemical parameters in the serum of patients with a diagnosis of acute subarachnoid hemorrhage. Transl Neurosci 14(1):20220311. https://doi.org/10.1515/tnsci-2022-0311